3D Graphics Techniques for Capturing and Inspecting Hyperspectral Appearance

Min H. Kim
Computer Science Department
KAIST
Daejeon, South Korea
Email: minhkim@kaist.ac.kr

Abstract—**Feature films and computer games exhibit stunning photorealistic computer imagery in motion. The challenges in computer graphics realism lie in acquiring physically accurate material appearance in a high spectral resolution and representing the appearance with perceptual faithfulness. While many approaches for true spectral rendering have been tried in computer graphics, they have not been extensively explored due to the lack of reliable 3D spectral data. Recently, a hyperspectral 3D acquisition system and viewing software have been introduced to the graphics community. In this paper, we review the latest acquisition and visualization techniques for hyperspectral imaging in graphics. We give an overview of the 3D imaging system for capturing hyperspectral appearance on 3D objects and the visualization software package to exploit such high-tech digital data.**

I. Introduction

Computer graphics has been developed in a spectrum ranging from feature films in the entertainment industry to scientific simulation in natural science and engineering. One of the important areas in graphics is to generate realistic visual images on a computer. In order to achieve high fidelity in computer graphics realism, it is essential to acquire 3D objects with a physically accurate system and to visualize them through a perceptually faithful workflow. In this paper, we give an overview of an advanced 3D imaging system to capture hyperspectral 3D material appearance with enhanced physical fidelity and an integrated visualization software package that enables inspecting hyperspectral measurement data with faithful color fidelity.

II. Related Work

This section surveys relevant techniques for high-fidelity acquisition and representation in graphics.

Color Characterization. Many 2D imaging techniques have been developed for measuring physically meaningful radiance with a digital camera [1]–[5]. They generally estimate a set of linear or non-linear transformations from device-dependent camera signals to device-independent coordinates of a color space such as CIEXYZ or CIELAB [6]. This is often called radiometric calibration or device characterization in cross-media reproduction. However, these calibration approaches allow metameric measurement errors due to limited bandwidth.

Imaging Spectroscopy. The spectral resolution of 2D imaging devices has been extended further recently, allowing us to capture spectral images with higher spatial and spectral resolution. 2D imaging spectroscopy allows us to measure such spectral properties as an image [7]–[14] whereas a spectrometer only measures the spectral power distribution of a single point of interest. Imaging spectroscopy techniques have been broadly used in many applications, such as military, biometrical imaging, and remote sensing. The form of spectral measurements is currently limited to 2D images.

Multispectral Rendering. Recently many approaches for true spectral rendering have been tried in 3D computer graphics to create physically accurate rendered images [15], [16]. However, such graphics rendering applications have rarely been exploited due to the lack of reliable 3D acquisition data with high physical fidelity. Therefore many scientific applications of spectral rendering in scientific studies have yet to be applied.

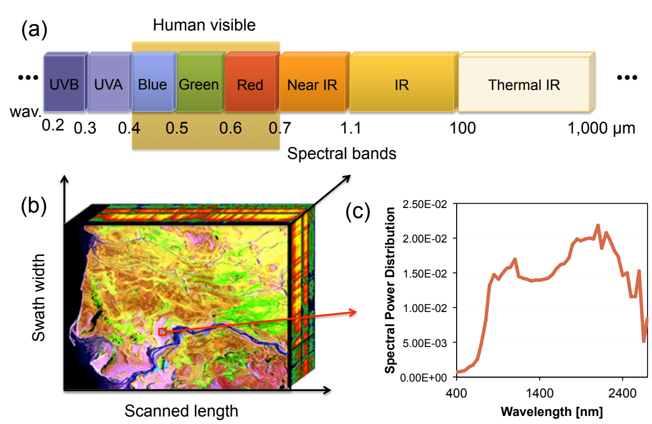

Fig. 1: *Schematic overview of hyperspectral imaging. (a) a spectral range of wavelengths around the visible spectrum, (b) an example of a hyperspectral image, (c) an example of a measured spectrum*

3D Imaging Spectroscopy. Kim et al. [17] bridge the gap between 2D image spectroscopy and 3D multispectral rendering by developing a scientific 3D scanning system that captures 3D spectral data at ∼12 nm resolution in the range of 359 nm to 1,003 nm. Kim et al. [18] also present an integrated software package to allow the user to inspect high dimensional spectral data visually and quantitatively. In this paper, the technical detail of the acquisition system is reviewed in Sec. III. The visualization software package is reviewed in Sec. IV.

III. Hyperspectral 3D Acquisition System

Hyperspectral imagers have been used for capturing visible/invisible radiometric properties of objects as an image. Figure 1 shows a general overview of hyperspectral imaging. (a) presents a spectral range of wavelengths around the visible spectrum. The left-hand-side of the human visible spectrum indicates the invisible range of ultraviolet energy, while the right-hand-side shows invisible infrared wavelengths. (b) visualizes the typical data structure of the spectral imaging data, where each pixel value contains the spectral power distribution (c) of the corresponding point in the image. Kim et al. [17] proposed a 3D imaging system that acquires point-to-point measurements of material appearance in a high spatial and spectral resolution. This section reviews the system briefly.

Spectral Imager. The 3D imaging system proposed by Kim et al. [17] consists of a custom-built hyperspectral imager, a triangulation-based laser scanner, a turntable gear, and xenon/ultraviolet light sources. See Figure 2 for a system overview. The spectral imager couples a coded aperture and a dispersive prism to solve the complex projection of spatial and spectral information. Solving the captured data in their imaging system is a typical under-determined problem. The system solves this with a sparsity-constrained optimization technique [19]. In particular, their camera system employs the multiple snapshots of the coded aperture and bandpass filters in order to enhance the spatial and spectral resolution simultaneously.

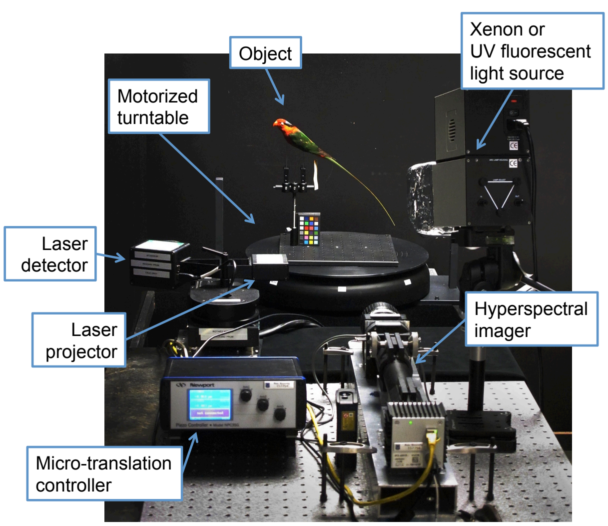

Fig. 2: *Overview of the 3D imaging spectroscopy system [17]. The system includes a custom-built hyperspectral imager, a laser scanner, a turntable, and xenon/ultraviolet light sources.*

Parallelization. The imaging system can achieve four megapixel resolution (2048×2048) with 53 channels (from 359 nm to 1,003 nm in ∼12 nm intervals). The designed system with the target spatial and spectral resolution requires a significant amount of memory to solve the sparsity-constrained optimization. The system first breaks the target spectrum to be solved into three bands with three bandpass filters and then parallelizes the computations into strips as shown in Figure 3.

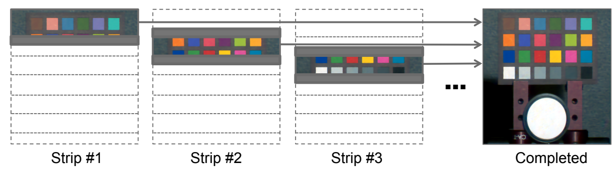

Fig. 3: *Computational parallelization of the system [17].*

The 3D model reconstruction workflow in the system is a two-part parallel process that includes geometric and radiometric streams. Both data processing streams are illustrated in Figure 4.

Geometric Process. The geometric process begins with step (a) in Fig. 4, where a range scanner captures a set of piecewise geometries—individual height-field meshes of the surface. Outliers and line-of-sight error are removed from the range images. Step (b) aligns the piecewise geometries into a single global coordinate system. Initial registration of the position and orientations is determined by the turntable calibration. The alignment is refined automatically using the iterative closest point (ICP) method [20]. They reduce scanner line-of-sight error using conformance smoothing [21]. In step (c) the scans are integrated into a single mesh. The integration is performed by the ball-pivoting algorithm [22] (computing a triangle mesh from an interpolated point cloud) and a volumetric merging technique [23] (computing a voxel grid within the bounding box). In step (d) they parameterize the integrated mesh for texture mapping. The surface is parameterized with respect to a 2D coordinate system, and texture coordinates are interpolated between mesh vertices. They partition the triangle mesh into height-field patches with a simple region-growing heuristic. Then, for each patch, an orthogonal projection in the direction that maximizes the projected patch area defines a mapping between the geometry and corresponding textures [24].

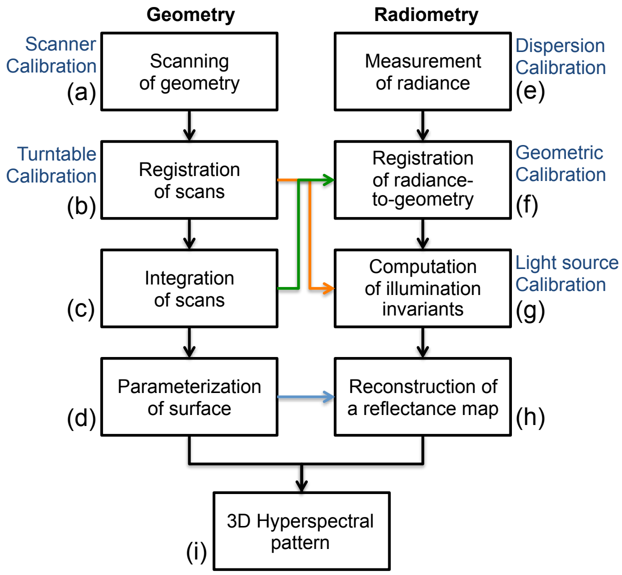

Fig. 4: *Parallel geometric and radiometric data processing pipeline for reconstructing a hyperspectral 3D reflectance model from piecewise scans and radiance maps in the system [17].*

Radiometry Process. The radiometric stream commences with the acquisition of piecewise hyperspectral radiance maps (step (e) in Fig. 4). In step (f), these radiance maps are aligned to the corresponding geometry by using the calibrated intrinsic and extrinsic parameters of the imager [25]. Then illumination invariant maps are computed as shadow maps, positive/negative normal maps, and depth maps to estimate the surface reflectance in step (g). In step (h), the final reflectance texture map is reconstructed by mapping the illumination invariant images onto the integrated, parameterized surfaces from (d). A texture synthesis method [24] is performed to complete the 3D hyperspectral data (i) of the target object.

IV. Hyperspectral 3D Imaging Software

There are several open-source programs to deal with various types of 3D data and enable various geometric operations [26]–[28]. However, these software packages are not configured to be extended to viewing hyperspectral 2D and 3D image data. Currently a software package introduced by Kim et al. [18] is a unique option that can handle various types of image modality from medical images to hyperspectral 3D models.

Hyperspectral Data Visualization. The main limitation in using hyperspectral images is that spectral data is highly dense and exceeds the human visual range. The proposed software package [18] represents hyperspectral data in two different stages. It first converts the high-dimensional spectral information to human visible color by projecting the original spectrum to trichromatic human vision using the CIE color matching functions [6]. However, as the spectral range of human vision is itself a subset of the electromagnetic spectrum sensible to the hyperspectral imager [17], the package provides an extra widget that visualizes hyperspectral spectrum information simultaneously with human-aware color rendering of 2/3D objects. When the user clicks on a point of interest, the widget shows the detail of the spectral measurements on a point-by-point basis. See Figure 5 for the user interface.

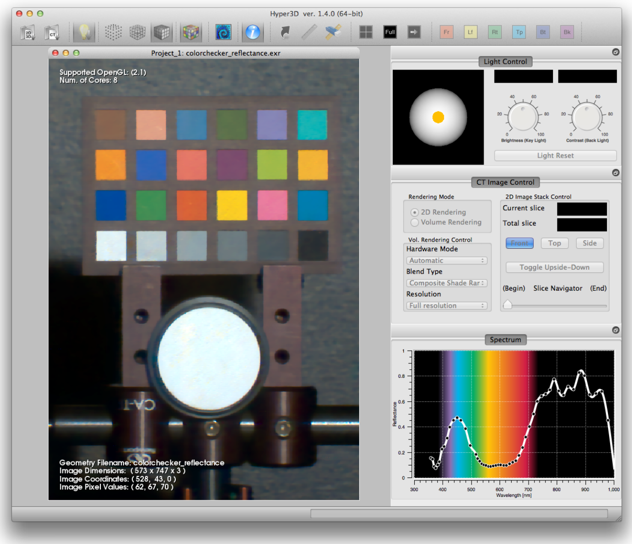

Fig. 5: *A screenshot of the integrated hyperspectral imaging software, proposed by [18]. The top-right widgets are for controlling rendering properties. The bottom-right widget represents the hyperspectral reading at a pixel of interest.*

V. Conclusion

We review computer graphics technologies developed for acquiring and inspecting hyperspectral 3D imaging data. While the reviewed system and software made the acquisition and visual inspection of high resolution spectral data possible, several challenges still remain. Long acquisition and processing times could be improved in the 3D imaging system [17]. Bidirectional reflectance properties in such high spectral resolutions could be explored as future work for both techniques.

Acknowledgment

The authors would like to thank Samsung Electronics and the National Research Foundation of Korea for grant (2013010165).

References

[1] M. R. Pointer, G. G. Attridge, and R. E. Jacobson, "Practical camera characterization for color measurement," in *PICS*, 2001, pp. 246–251.

[2] K. Barnard and B. V. Funt, "Camera characterization for color research," *Color Res. Appl.*, vol. 27, no. 3, pp. 153–164, 2002.

[3] C. Normand, P. Fornaro, and R. Gschwind, "Automated digital camera sensor characterization," in *SPIE/IS&T Electronic Imaging*, vol. 6502, 2007.

[4] M. H. Kim and J. Kautz, "Characterization for high dynamic range imaging," *Computer Graphics Forum (Proc. EUROGRAPHICS)*, vol. 27, no. 2, pp. 691–697, 2008.

[5] M. H. Kim and H. Rushmeier, "Radiometric characterization of spectral imaging for textual pigment identification," in *Proc. International Symposium on Virtual Reality, Archaeology and Cultural Heritage (VAST 2011)*. Tuscany, Italy: Eurographics, 2011, pp. 57–64.

[6] CIE, "Colorimetry," Commission Internationale de l'Eclairage (CIE), Vienna, CIE Pub. 15.2, 1986.

[7] W. L. Smith, D. K. Zhou, F. W. Harrison, H. E. Revercomb, A. M. Larar, H. L. Huang, and B. Huang, "Hyperspectral remote sensing of atmospheric profiles from satellites and aircraft," in *Proc. SPIE*, vol. 4151, 2001, pp. 94–102.

[8] C. M. Stellman, F. M. Olchowski, and J. V. Michalowicz, "War horse (wide-area reconnaissance: hyperspectral overhead real-time surveillance experiment)," in *Proc. SPIE*, vol. 4379, 2001, pp. 339–346.

[9] M. E. Gehm, M. S. Kim, C. Fernandez, and D. J. Brady, "High-throughput, multiplexed pushbroom hyperspectral microscopy," *Opt. Express*, vol. 16, no. 15, pp. 11 032–11 043, 2008.

[10] T. H. Pham, F. Bevilacqua, T. Spott, J. S. Dam, B. J. Tromberg, and S. Andersson-Engels, "Quantifying the absorption and reduced scattering coefficients of tissuelike turbid media over a broad spectral range with noncontact fourier-transform hyperspectral imaging," *Appl. Opt.*, vol. 39, pp. 6487–6497, 2000.

[11] A. Wagadarikar, R. John, R. Willett, and D. J. Brady, "Single disperser design for coded aperture snapshot spectral imaging," *Appl. Opt.*, vol. 47, no. 10, pp. B44–B51, 2008.

[12] A. A. Wagadarikar, N. P. Pitsianis, X. Sun, and D. J. Brady, "Video rate spectral imaging using a coded aperture snapshot spectral imager," *Opt. Express*, vol. 17, no. 8, pp. 6368–6388, 2009.

[13] D. Kittle, K. Choi, A. Wagadarikar, and D. J. Brady, "Multiframe image estimation for coded aperture snapshot spectral imagers," *Appl. Opt.*, vol. 49, no. 36, pp. 6824–6833, 2010.

[14] M. E. Gehm, R. John, R. Willett, T. Schultz, and D. Brady, "Single-shot compressive spectral imaging with a dual disperser architecture," *Opt. Express*, vol. 15, pp. 14 013–14 027, 2007.

[15] K. Devlin, A. Chalmers, A. Wilkie, and W. Purgathofer, "Tone reproduction and physically based spectral rendering," *Eurographics 2002: State of the Art Reports*, pp. 101–123, 2002.

[16] M. Pharr and G. Humphreys, *Physically Based Rendering: From Theory to Implementation*. San Francisco, CA, USA: Morgan Kaufmann Publishers Inc., 2004.

[17] M. H. Kim, T. A. Harvey, D. S. Kittle, H. Rushmeier, J. Dorsey, R. O. Prum, and D. J. Brady, "3d imaging spectroscopy for measuring hyperspectral patterns on solid objects," *ACM Transactions on Graphics (Proc. SIGGRAPH 2012)*, vol. 31, no. 4, pp. 38:1–11, 2012.

[18] M. H. Kim, H. Rushmeier, J. ffrench, and I. Passeri, "Developing open-source software for art conservators," in *VAST12: The 13th International Symposium on Virtual Reality, Archaeology and Intelligent Cultural Heritage*. Brighton, England: Eurographics Association, 2012, pp. 97–104.

[19] J. Bioucas-Dias and M. Figueiredo, "A new twist: two-step iterative shrinkage/thresholding for image restoration," *IEEE Trans. Image Processing*, vol. 16, no. 12, pp. 2992–3004, 2007.

[20] P. J. Besl and N. D. McKay, "A method for registration of 3-D shapes," *IEEE Transactions on Pattern Analysis and machine Intelligence*, vol. 14, no. 2, pp. 239–258, Feb. 1992.

[21] F. Bernardini, H. E. Rushmeier, I. M. Martin, J. Mittleman, and G. Taubin, "Building a digital model of michelangelo's florentine pietà," *IEEE Computer Graphics and Applications*, vol. 22, no. 1, pp. 59–67, 2002.

[22] F. Bernardini, J. Mittleman, H. E. Rushmeier, C. T. Silva, and G. Taubin, "The ball-pivoting algorithm for surface reconstruction," *IEEE Trans. Vis. Comput. Graph*, vol. 5, no. 4, pp. 349–359, 1999.

[23] M. Callieri, P. Cignoni, F. Ganovelli, C. Montani, P. Pingi, and R. Scopigno, "VCLabs tools for 3D range data processing," in *International Symposium on Virtual Reality, Archaeology and Intelligent Cultural Heritage*, D. Arnold, A. Chalmers, and F. Niccolucci, Eds. Brighton, United Kingdom: Eurographics Association, 2003, pp. 13–22.

[24] F. Bernardini, I. M. Martin, and H. E. Rushmeier, "High-quality texture reconstruction from multiple scans," *IEEE Trans. Vis. Comput. Graph.*, vol. 7, no. 4, pp. 318–332, 2001.

[25] R. Y. Tsai, "A versatile camera calibration technique for high-accuracy 3D machine vision metrology using off-the-shelf TV cameras and lenses," *IEEE Journal of Robotics and Automation*, vol. 3, pp. 323–344, 1987.

[26] P. Cignoni, M. Corsini, and G. Ranzuglia, "Meshlab: an open-source 3D mesh processing system," *ERCIM News*, vol. 2008, no. 73, 2008.

[27] Alice, "Graphite," http://alice.loria.fr/index.php/software/3-platform/22-graphite.html, 2008.

[28] J. Möbius and L. Kobbelt, "Openflipper: An open source geometry processing and rendering framework," in *Curves and Surfaces*, ser. Lecture Notes in Computer Science, vol. 6920. Springer, 2010, pp. 488–500.